University of Huddersfield Repository

Arebi, Lufti, Gu, Fengshou and Ball, Andrew

Rotor Misalignment Detection using a Wireless Sensor and a Shaft Encoder

Original Citation

Arebi, Lufti, Gu, Fengshou and Ball, Andrew (2010) Rotor Misalignment Detection using a Wireless Sensor and a Shaft Encoder. In: Future Technologies in Computing and Engineering: Proceedings of Computing and Engineering Annual Researchers' Conference 2010: CEARC'10. University of Huddersfield, Huddersfield, pp. 6-13. ISBN 9781862180932

This version is available at http://eprints.hud.ac.uk/id/eprint/9307/

http://eprints.hud.ac.uk/

ROTOR MISALIGNMENT DETECTION USING A WIRELESS SENSOR AND A SHAFT ENCODER

Lutfi Arebi, Fengshou Gu and Andrew Ball

University of Huddersfield, Queensgate, Huddersfield HD1 3DH, UK

ABSTRACT

Mechanical systems such as motors, pumps, engines, and turbine are all operating based on different shafts. Due to unexpected operating conditions, various faults such as cross-sectional cracks, looseness and misalignment may occur during their service life. This paper presents the analysis of collected signals from a wireless sensor and a shaft encoder and compares their responses under different degrees of shaft misalignment. The results have shown that the wireless sensor outperforms the encoder in detecting small shaft misalignment.

Keywords Wireless Sensor, Vibration, Misalignment, Encoder, Instantaneous Angular Speed (IAS)

1   INTRODUCTION

The most common cause of machine vibration is rotor misalignment after imbalance, which leads additional dynamic load and accelerate machine deterioration. This type of vibration is often from reactive forces in the couplings between two rotating shafts. Understanding and practicing the fundamentals of rotating shaft parameters is the first step in reducing this unnecessary vibration, reducing maintenance costs and increasing machine uptime. In industry, 30% of a machine's downtime is due to the poorly aligned machines [1]. Misalignment is estimated to cause over 70% of rotating machinery's vibration problems [3]. Hence, an in-depth study and an accurate knowledge on the vibration characteristics is very helpful in understanding and diagnosing the rotor misalignment to avoid any failures or damages that may arise [2].

There are various factors such as differential thermal growth of machines, asymmetry in applied loads, unequal foundation settlement, etc., which disturb the alignment condition of a machine [2]. Despite the rapid increase in the understanding of rotor dynamics, no satisfactory analysis explains the range of observed phenomena [1]. Vance [4] and Goodman [5] observed that misalignment is present due to improper machine assembly and sometimes, the thermal distortion of the bearing housing supports, resulting in abnormal rotating preload. However, a perfect alignment between the driving and driven shafts cannot be attained. Gibbons [6] first derived the misalignment reaction forces from those generated in different types of couplings.

Xu and Marangoni [7] showed analytically that the vibration due to coupling misalignment mainly occur at the even multiples of the rotor speed. Sekhar and Prabhu [8] numerically evaluated the effect of coupling misalignment on the vibration response of the rotor. They suggested 2X vibration response as a characteristic signature of misaligned shafts. Dewell and Mitchell [11] showed experimentally that 2X and 4X vibration components are largely dependent upon coupling misalignment.

Lee [9] derived a model for the flexible coupling–rotor–ball bearing system, including reaction loads from deformations of rolling elements of bearing and coupling elements as the misalignment effects. From orbital analysis, anisotropy of bearing stiffness was suggested as the misalignment indicator. The other approach often used to simulate misalignment effect in rotor system is from kinematics of the couplings.

Piotrowski [10] concluded that vibration due to misalignment is usually characterized by a 2X running speed component and high axial vibration levels. When a misaligned shaft is supported by rolling-element bearing, these characteristic frequencies may also appear. Tejas and Ashish [2] found from the measured forces that the presence and type of misalignment (parallel and angular misalignment) has significant influences on the harmonic content of the misalignment excitation forces.

From the literature, it is clearly proven that misalignment produces high vibration levels in bearings. It is influenced by the machine speed and the stiffness of the coupling. e.g., rubber couplings are more tolerant and tend to produce less amount of vibration.

In general, the majority of misalignment studies in the past are theoretical whereas experimental investigations are relatively limited. The theoretical studies are often investigated with simplified assumptions. The outcome of these studies may not be accurate, since in practice there are many more sources of observed vibration characteristics in an actual rotor system. Moreover, all of these studies used wired accelerometer which is usually attached to the bearings housing. However, this work presents a comparison between IAS waveform from encoder and a newly designed wireless accelerometer waveform to investigate shaft misalignment. As the wireless sensor is mounted directly on the shaft, the true dynamics of the shaft can be recorded. In addition, it focuses specifically on experimental study of misaligned coupled rotors supported by ball and roller bearings.

2   WIRELESS SENSOR DEVELOPMENT

The wireless accelerometer node used in this research was developed based on a MEMS accelerometer ADXL202AE with a duty cycle output which can be conditioned conveniently to work wirelessly by the transmitter and receiver modules. The accelerometer is able to measure positive and negative absolute accelerations of ± 2g. The duty cycle period is adjustable from 0.5 ms to 10 ms via a single resistor (R_{SET}) [12]. The duty cycle outputs are available from X_{OUT} and Y_{OUT} pins. Moreover, the analogue output can be reconstructed by filtering the duty cycle outputs.The bandwidth of the ADXL202 can be set from 10 Hz to 5 kHz via capacitors C_X and C_Y as shown in Figure 1[12].
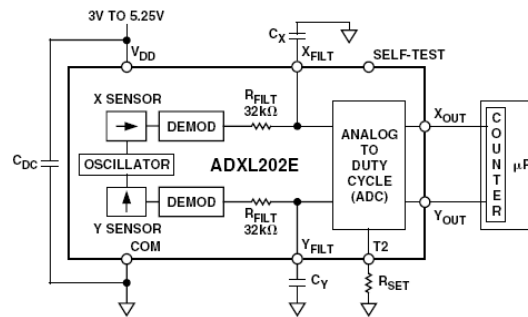

Figure 1 Accelerometer block diagram [12]

The first step in the design is to select the period of duty cycle (T) so that the analogue output can be reconstructed. According to the specifications of the accelerometer, T should be in the range of from 0.5ms to 0.9ms.

The duty cycle period was adjusted to 0.544ms by the resistor (RSET=68 KΩ). Therefore, the frequency of DCS was 1.838 kHz. The bandwidth of the accelerometer was set to 500 Hz by selecting capacitors C_x and C_y to be 0.01 µF. Sensitivity of the wireless accelerometer has been computed $(S_a) = 27.98165 \, mV/ms^{-2}$ [12].

To benchmark the performance of wireless sensor, an incremental shaft encoder, shown in Figure 2, is used in this experiment to measure IAS of the same shaft. The device provides a 1000 electrical pulse train per revolution from which IAS can be extracted using a soft time counting approach[14,15]. It has following main steps:

1) Calculate the time difference variation Δt of the encoder signal as shown in Figure 3.
2) The change in angular displacement Δθ can be computed knowing that the encoder generates 1000 pulses per revolution as:

$$\Delta\theta = \frac{2\pi}{1000} = 0.0063 \ (rad) \tag{1}$$

3) From step 1) and 2) the IAS can be calculated by:

$$\omega(t) = \frac{\Delta\theta}{\Delta t(t)} \ (rad/sec) \tag{2}$$
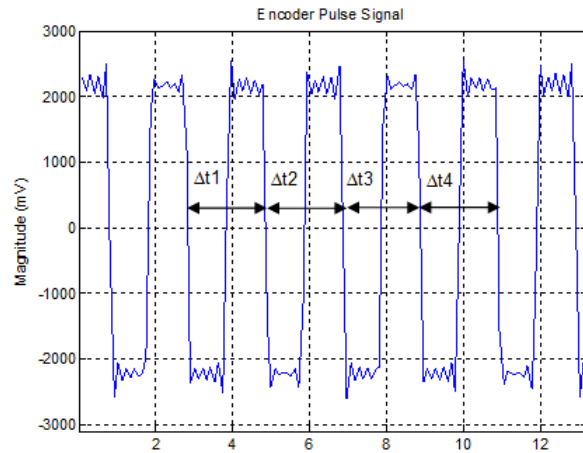
Figure 2: Incremental Shaft Encoder [14]

Figure 3: Raw signal from encoder

3   TEST FACILITY AND METHOD

A bearing test rig, shown in Figure 4, was employed in this experimental study. It consists of a 3-phase electrical induction motor to provide a prime power source and a DC generator to apply load to the motor. The motor is connected to the generator through two pieces of shafts, which are connected by three pairs of flexible couplings and supported by bearings in two bearing housings. The construction allows the study of different types of misalignments such as angular and parallel misalignments in different parts of the shaft system. The wireless accelerometer was mounted directly on the shaft connecting to the shaft of the motor while an encoder was mounted at the rotor end of the induction motor as shown in Figure 4 and 5. The test rig can run in a speed range from 60rpm to 1420rpm.
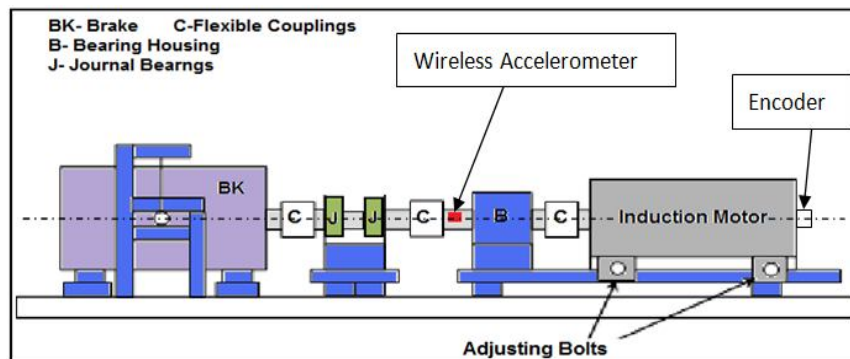

Figure 4: Test rig schematic and wireless sensor placement

The wireless accelerometer is mounted directly on the second shaft. As depicted in Figure 5. The principal axis of the sensor is along the tangential direction as indicated in the left drawing of Figure 5.
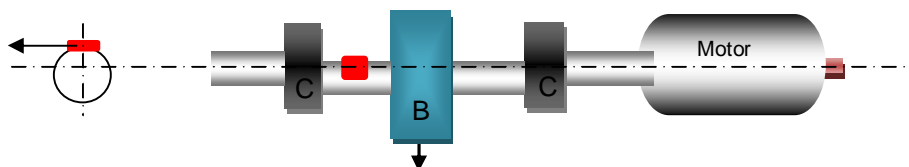

Figure 5: Schematic diagram of misaligned shaft

Figure 6 summarizes the procedure of the test. The test was conducted by comparing the results of IAS signals extracted from the encoder and the acceleration from the wireless accelerometer after each change of the alignment condition. Using the dial indicator, different degrees of misalignment of the second shaft is adjusted to designed values. The couplings installed in this test rig are flexible couplings. The misalignment type used for this test is a parallel misalignment in the horizontal direction.
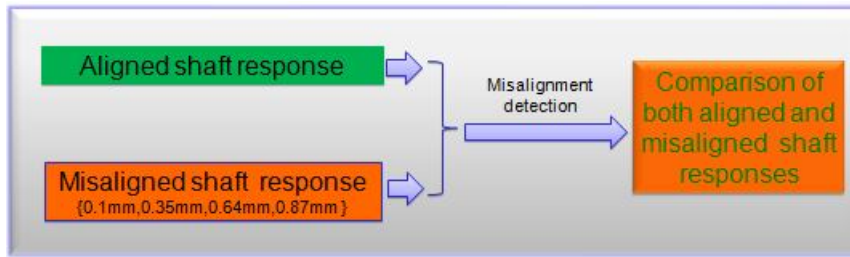
Figure 6: Misalignment test procedure

The steps of the test conducted are:

- Wireless accelerometer is mounted directly on the second shaft.
- The received signal from wireless sensor is fed to a Law Pass Filter (LPF) to reconstruct the analogue form of the signal. The output of LPF is connected to a high performance Data Acquisition System (DAS).
- The signal from encoder is conditioned and also connected to the DAS simultaneously. It comprises of 1000 pulses per revolution from which the IAS is generated.
- The test rig then ran under different speeds at a fixed load (50%) when it is in healthy condition with minimal misalignment between different shafts. The data was collected from both the wireless accelerometer and the encoder.
- Using a dial indicator, the first misaligned shaft is applied. The test rig then ran for different speeds and the data was collected. This step is repeated for different misalignments.
- The collected data is then analysed using a Matlab program.

While the wireless accelerometer was mounted on the shaft, the receiver, which receives duty cycle signal of the sensor, was connected to Sallen-Key second order active low pass filter with a cut-off frequency of 131.5 Hz. This filter is designed to filter the duty cycle signal in order to reconstruct the analogue form of acceleration signals. Then, the filtered signals are fed to a high speed data acquisition system. The sampling frequency was set to 96 kHz to capture more details in the waveform for further analysis. The recorded signals were processed using a program developed in Matlab.

4   RESULTS AND DISCUSSION

Figure 7 shows typical waveforms for different misalignments and shaft speeds. As illustrated in the top row of the figure 7(a), the outputs of the wireless sensor for healthy case show clear periodic oscillations respective to shaft fundamental period. This may be due to inevitable misalignment from other shafts in the system. In contrast, cases with high degree of misalignments exhibit only a small increase in waveform amplitudes. Nevertheless this small increase can be used to detect the occurrence of misalignments. On the other hand, the IAS waveform from the encoder with high degree of misalignments exhibit increase in waveform amplitudes whereas with low degree of misalignment only small decrease in waveform amplitudes as illustrated in Figure 7(b).

To compare waveforms more accurately, the root mean square (RMS) values are calculated over different misalignment cases. As shown in Figure 8, RMS amplitudes are clearly higher at faster speeds and greater misalignments. This demonstrates that RMS values of wireless outputs can be based on to differentiate the high misalignment cases from the healthy case and between different degrees of misalignment. Whereas the RMS values of encoder outputs can be used only to differentiate the high misalignment case from healthy case.

In addition, Figure 8 (Wireless) also shows that there are several low amplitude points in the trends with respect to different speeds and different degrees of misalignments. Especially, in the low speed and low misalignment cases, the trends behave very irregularly. In contrast, Figure 8 (Encoder) shows low amplitude points for low degrees of misalignment cases at different speeds. Obviously, this is not consistent with theoretical prediction. To understand this uncertainty, a spectrum analysis is carried out.
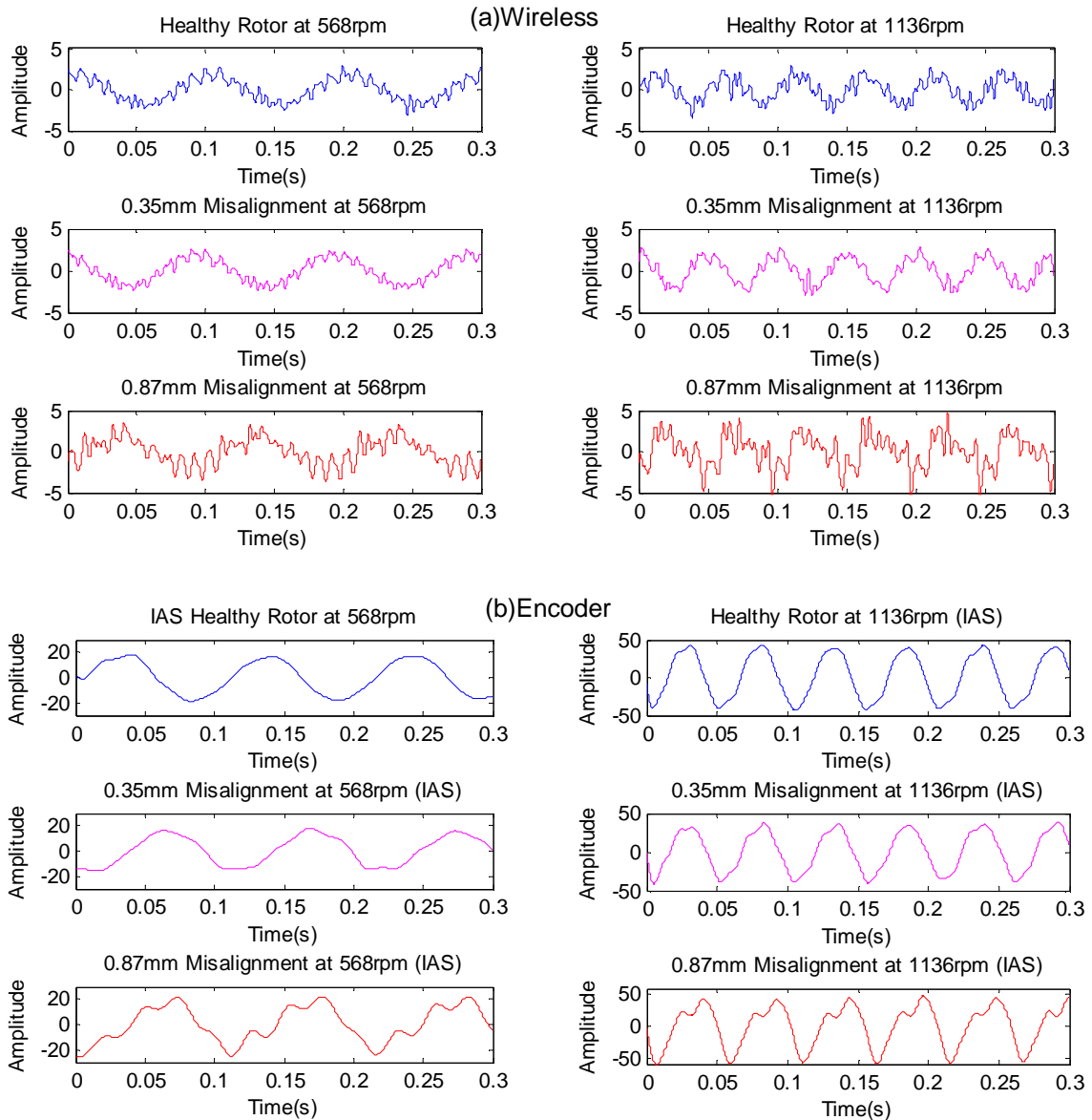
Figure 7: a) Wireless sensor b) Encoder waveforms for different shaft conditions at higher and lower speeds

Figure 9 shows typical spectra for the healthy case and the case with the highest misalignment over different speeds. For the healthy case, the shaft frequency is the dominant component and more components in higher order harmonics can be observed at higher speed. For the misalignment case, most of spectral amplitudes become higher and more harmonic components appear as the speed increases.

However, it was found that the shaft frequency produces a modulation to the component at 100Hz in the case of wireless sensor signal. Further investigation show that the 100Hz component is due to the imbalance of power supply between three phases. The interactions between the higher order harmonics of the shaft frequency and the sidebands of 100Hz may lead to irregular fluctuation in the spectral amplitudes over speed and misalignment. In particular, if the two components appear at a same frequency value but their phases are opposite, the amplitude becomes lower. However, the amplitude becomes very high if the two components have the same phases. As shown in Figure 9, all of the irregular amplitudes appear at intersects between the higher order harmonic lines (illustrated by blue dotted lines), and the sideband lines (illustrated by pink dotted lines). Therefore, it can be confirmed that the irregularities in the speed and misalignment trends are due to the modulation, careful analytical thoughts must be considered for using the amplitude to generate differences between different cases for fault diagnosis.
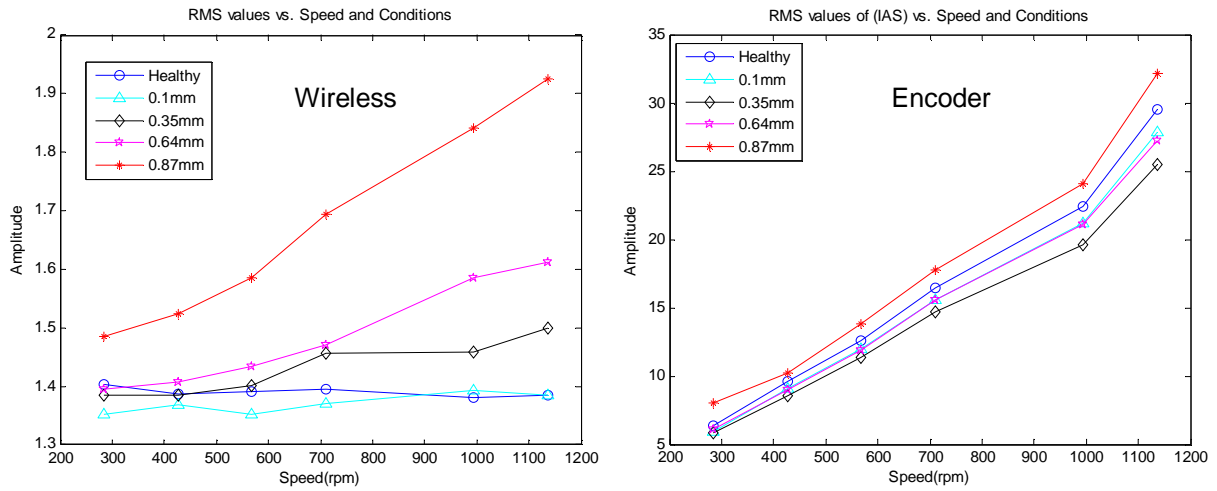
Figure 8: Waveform RMS values versus speeds and misalignments.

Nevertheless it has been observed from the spectra of wireless that amplitudes at shaft frequency under low speeds show a significant difference between the healthy and the misaligned case. The amplitudes for all the test cases are then extracted for detecting low misalignment cases. Whereas the spectra of IAS amplitudes at low speeds show very small irregular difference between healthy and misaligned case. In contrast, the amplitudes at high speeds show irregular significant difference.
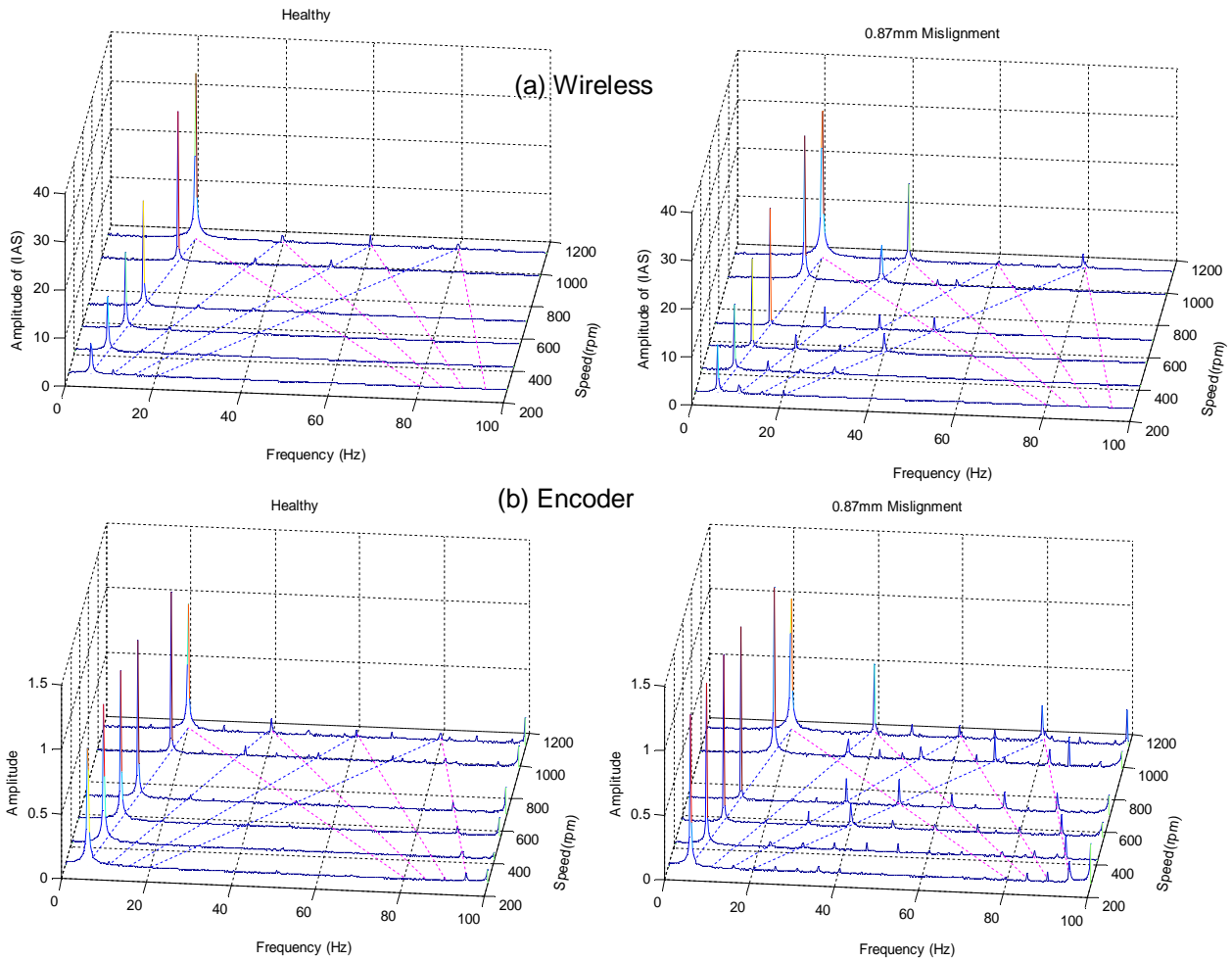

Figure 9: Spectra versus speed for healthy case

As shown in Figure 10, misalignment cases below 1000rpm can be separated from the healthy case, proving that the shaft spectral amplitude of wireless sensor is capable of detecting a small fault at low speeds. In contrast, the IAS is capable of detecting the higher degree of misalignment only (above 0.87mm).

However, in the case of wireless, as shown in Figure 10, using the shaft frequency amplitude alone cannot yield a proper discrimination between different misalignments. In order to compensate for this, perhaps the results in Figure 8 have to be employed. It means that combining the shaft frequency amplitudes with waveform RMS values can give both detection and diagnosis results for most of the faulty cases.
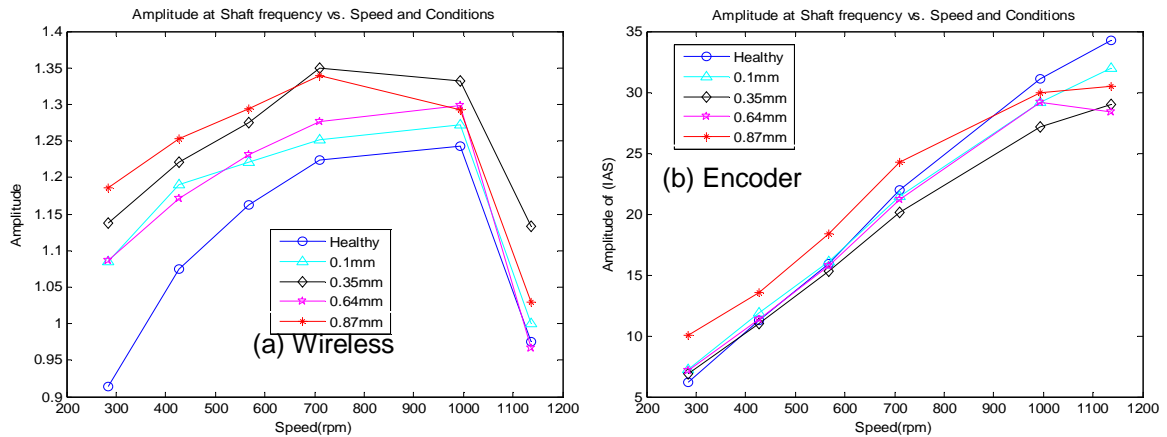

Figure 10: Detection performance based on shaft frequency component

5   CONCLUSIONS

From this study, the low cost and low power consumption wireless accelerometer developed in this study can be used to measure the dynamics of a rotating shaft directly. Compared with IAS signal from the encoder, the wireless sensor produces more accurate results in monitoring a rotating shaft with different degrees of misalignment. In particular, the difference in the amplitude of rotational components can be used to separate the healthy case from different degrees of misalignments below 1000rpm. In association with waveform RMS, it can also produce diagnostic results for higher misalignment cases. However, RMS values from IAS waveforms show that irregular amplitude difference between healthy and misaligned above 300rpm except for the higher degree of misalignment. Also, IAS spectral amplitudes show that the higher degree of misalignment can be detected only below 900 rpm.

REFERENCES

1. V. Hariharan, PSS. Srinivasan, Kongu Engg, (2009): 'Vibration analysis of misaligned shaft –ball bearing system', Indian Journal of Science and Technology, Vol.2 No. 9, ISSN: 0974- 6846.

2. TejasH. Patel, AshishK. Darpe, (2009): 'Experimental investigations on vibration response of misaligned rotors', Mechanical Systems and Signal Processing, Vol.23, No 7, pp 2236–2252.

3. Bognatz S.R., (1995): 'Alignment of critical and non critical machines', Orbit 23–25.

4. Vance JM (1988): 'Rotor dynamics of Turbomachinery'. New York, John Wiley & Sons.

5. Goodman MJ (1989): 'Dynamics of rotor – bearing systems', London, Unwin Hyman Ltd.

6. Gibbons C.B., (1976): 'Coupling misalignment forces', Proceedings of the 5th Turbo Machinery Symposium, Gas Turbine Laboratory, Texas A & M University, pp. 111–116.

7. Xu M., R. Marangoni RD, (1994a): 'Vibration analysis of a motor-flexible coupling-rotor system subjected to misalignment and unbalance Part I: Theoretical model and analysis', Journal of Sound and Vibration, 176(5), 663–679.

8. Sekhar A.S., Prabhu B.S., (1995): 'Effects of coupling misalignment on vibration of rotating machines', Journal of Sound and Vibration 185, 655–671.

9. Lee Y.S., Lee C.W., (1999): 'Modelling and analysis of misaligned rotor–ball bearing systems', Journal of Sound and Vibration 224 17–32.

10. Piotrowski J., 'Shaft Alignment Handbook', Marcel Dekker Inc., New York, (1995).

11. Dewell DL and Mitchell LD, (1984): 'Detection of a misaligned disk coupling using spectrum analysis'. ASME Trans. J. Vibration, Acoustics, Stress & Reliability Design. 106, 9-16.

12. Analog Devices, Inc, ADXL202E Catalogue, at http://www.analog.com, (2000).

13. David M. Alter, (2008): 'Using PWM Output as a Digital-to-Analog Converter on a TMS320F280x Digital Signal Controller, DSP Applications-Semiconductor Group', Texas Instruments, SPRAA88A.

14. Hengstler, Inc. TECHNICAL DATASHEET Incremental Encoder RI32 http://www.hengstler.com/en/products/shop.php,catID=1011&artID=34.

15. Y Li, F. Gu, A. D. Ball and, N. Bennett (2004), "The measurement of Instantaneous Angular Speed", Mechanical Systems and Signal Processing, Vol. 19, No 4, pp. 786-805.

16. Lutfi Arebi, Yibo Fan, Fengshou Gu and Andrew Ball, (2010):' Investigation of Wireless Sensor Directly Deployed on Rotating Shaft and Its Potential for Machinery Condition Monitoring', Proc. Of COMADEM 2010, Japan.